J Nanostruct Chem (2016) 6:103–109
DOI 10.1007/s40097-015-0184-8

ORIGINAL RESEARCH

Structure, energetics, spectral and electronic properties of $B_3N_3C_{54}$ heterofullerene

Ambrish Kumar Srivastava[1] · Sarvesh Kumar Pandey[2] · Neeraj Misra[1]

Received: 27 September 2015 / Accepted: 11 November 2015 / Published online: 22 January 2016

Abstract Introduction of heteroatoms into C_{60} fullerene leads to enhance its physical and chemical properties in one way or other. In this paper, we have studied C_{60} fullerene in which one of C_6 hexagons is replaced by B_3N_3 using density functional theory at B3LYP/6-31G(d) level. The resulting heterofullerene $B_3N_3C_{54}$ closely mimics the structure of C_{60} in which the polar BN bonds are weaker than covalent CC bond. The stabilization energy of $B_3N_3C_{54}$ is found to be 5.35 eV. The vibrational infrared and Raman spectra of $B_3N_3C_{54}$ have been calculated and compared with that of C_{60}. The substitution results in a number of additions peaks including the strongest peak corresponding to BN stretching due to charge transfer from B to N atoms. The NMR chemical shifts of $B_3N_3C_{54}$ have also been computed using GIAO approach. The electronic parameters and DOS spectrum of $B_3N_3C_{54}$ have been compared with C_{60} and their degenerate molecular orbitals have been plotted. The HOMO–LUMO energy gap of $B_3N_3C_{54}$ is lowered by 0.1 eV as compared to C_{60}.

Keywords Heterofullerene · BN substitution · Vibrational spectra · HOMO–LUMO gap · Density functional theory

✉ Neeraj Misra
neerajmisra11@gmail.com

[1] Department of Physics, University of Lucknow, University Road, Lucknow, Uttar Pradesh 226007, India

[2] Department of Chemistry, Indian Institute of Technology Kanpur, Kanpur, Uttar Pradesh 208016, India

Introduction

Carbon forms a variety of nanostructures in which C_{60} fullerene is particularly remarkable due to its finite size and for many technological applications [1, 2]. The electronic properties of fullerenes have been found to be affected by doping of atoms [3] and molecule [4]. Introduction of heteroatoms into C_{60} fullerene leads to distinguished physical and chemical properties which make them promising materials for some unique applications [5–7]. In particular, BN substituted C_{60} cages have been studied several times [8–14]. Esfarjani et al. [8] have studied the band structure and chemical bonding in BNC_{58} heterofullerenes and its electronic spectra are studied by Chen et al. [9]. Krainara et al. [10] and Siddiqui et al. [11] have studied the interaction of BNC_{58} with adenine Cu(II) complexes and suggested that this heterofullerene is capable to differentiate electronically equivalent tautomers of DNA base pair. A systematic study on $C_{60-2x}(BN)_x$ ($x = 1$–7) hybrid fullerene has been performed by Pattanayak et al. [12] and subsequently extended up to $C_{12}B_{24}N_{24}$ [13]. Anafcheh et al. [14] have recently performed NMR calculations on $C_{60-2x}(BN)_x$ ($x = 1$, 2, 3, 6, 9, 12, 15, 18, 21, and 24) using density functional theory (DFT). The uniqueness of BN doped C_{60} is due to the fact that polar BN bond is analogous to covalent CC bond in many aspects [15]. For instance, borazine ($B_3N_3H_6$) shows a great similarity with that of benzene (C_6H_6) [16–18] and hence, it is regarded as inorganic benzene. However, it is noticeable that the polarity of the BN bond causes borazine to show a reactivity pattern different from that of benzene. For instance, benzene is aromatic, but borazine is probably non-aromatic. Furthermore, BN analogs of many carbon nanostructures such as boron-nitride nanotubes, boron-nitride nanosheets, etc., have been well studied and reported.

One might, therefore, expect that BN substituted C_{60} fullerenes are structurally analogous to pure C_{60}. Therefore, it should be interesting to analyze the effect of this substitution on the physical and chemical properties of C_{60}. In this paper, we report density functional theory-based study on a substituted C_{60} in which one of C_6 hexagons is replaced by B_3N_3. Spectral properties such as infrared, Raman and NMR spectra provide the signature of the molecular structure. Therefore, we analyze the spectral features of $B_3N_3C_{54}$ and compare it with C_{60}. Moreover, the electronic properties of $B_3N_3C_{54}$ heterofullerene have been explored and compared with those of C_{60}.

Computational methods

The study was performed using density functional theory (DFT) method as implemented in Gaussian 09 program [19]. All structures considered in this were fully optimized without any symmetry constraint using B3LYP exchange–correlation functional [20, 21] with 6-31G(d) basis set. The B3LYP scheme has already been used in our previous study on LiF nanostructures [22]. More recently, B3LYP/6-31G(d) level has been proved to yield accurate results in case various fullerene derivatives [23]. Vibrational frequency calculations and natural population analysis (NPA) have been carried out within the same computational scheme. In a recent study, we have noticed that NPA charges are more reliable than many other population schemes [24].

Results and discussion

Structure and energetics

The optimized structure of $B_3N_3C_{54}$ along with C_{60} is displayed in Fig. 1. One can note that the structure of $B_3N_3C_{54}$ closely resembles that of C_{60} in which one of C_6 hexagons is replaced by B_3N_3, but its symmetry is reduced to C_3 point group. To get further insights, we have separately optimized C_6 and B_3N_3. After optimization, we have found that they are almost similar in structure, also shown in Fig. 1. Both possess D_{3h} symmetry and equalized bond lengths, 1.358 Å for B–N and 1.327 Å for C–C. The NPA charges on B and N atoms in B_3N_3 are $+1.04e$ and $-1.04e$, respectively, which suggest polarity of BN bonds. In Table 1, we have collected the bond lengths of hexagon–hexagon and hexagon–pentagon in $B_3N_3C_{54}$ and C_{60}. Evidently, the B–N bond lengths increase to 1.437 Å and 1.478 Å in hexagon–hexagon and hexagon–pentagon edges which indicate that B–N bonds of the substituted fullerene are weaker than those of free B_3N_3. Furthermore, the difference of B–N and C–C bond lengths is significantly increased. This may be expected due to redistribution of charges on B and N atoms in $B_3N_3C_{54}$. For instance, NPA charges on B and N atoms in $B_3N_3C_{54}$ are $+1.02e$ and $-0.88e$, respectively. One can note that the polarity of BN bonds reduces in $B_3N_3C_{54}$ which weakens the bond increasing its bond length.

The formation of $B_3N_3C_{54}$ involves two processes: the removal of C_6 hexagon from C_{60} and then, inclusion of B_3N_3 hexagon at the same place. The corresponding stabilization energy can be calculated by,

$$\Delta E = E[B_3N_3C_{54}] + E[C_6] - E[C_{60}] - E[B_3N_3]$$

where E[..] represents the total electronic energy of respective species including zero point correction. The calculated E values are -2296.5835, -2286.1742, -238.8580, and -228.2520 a.u. for $B_3N_3C_{54}$, C_{60}, B_3N_3, and C_6, respectively, at B3LYP/6-31G(d) level. Therefore, ΔE value is found to be 5.35 eV which is positive and large enough to establish that the $B_3N_3C_{54}$ heterofullerene is kinetically stable.

Spectral properties

We have calculated vibrational infrared, Raman and NMR spectra of $B_3N_3C_{54}$ and compared with those of C_{60}. The

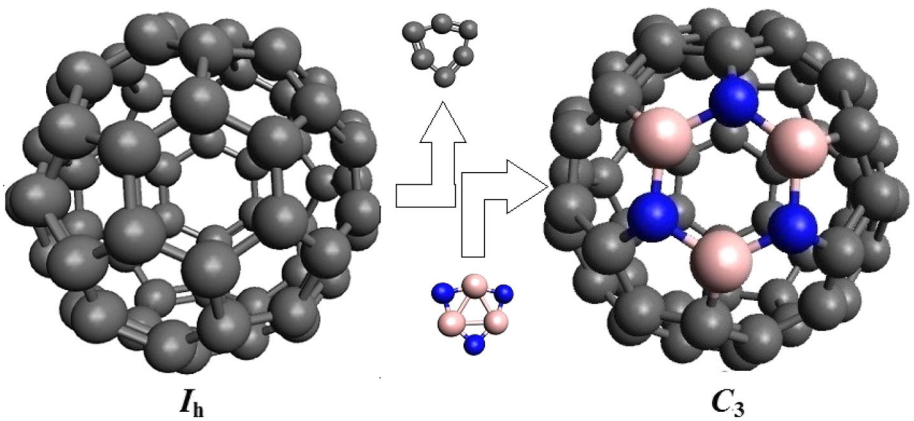

Fig. 1 Equilibrium structures of C_{60} (*left*) and $B_3N_3C_{54}$ (*right*) calculated at B3LYP level

Table 1 Main bond lengths (in Å) of $B_3N_3C_{54}$ and C_{60} at B3LYP/6-31G(d) level

System (bond length)	Hexagon–hexagon	Hexagon–pentagon
C_{60} (C–C)	1.395	1.453
$B_3N_3C_{54}$ (B–N)	1.437	1.478
(B–C)	1.526	1.526
(N–C)	1.434	1.434

vibrational frequency calculations performed on $B_3N_3C_{54}$ heterofullerene reveal all real and positive values. This suggests that $B_3N_3C_{54}$ belongs to at least some local minimum in the potential energy surface. The calculated vibrational infrared and Raman spectra of $B_3N_3C_{54}$ and C_{60} are depicted in Fig. 2. For *N*-polyatomic systems, there are 3*N*-6 normal modes of vibration. Due to extremely high symmetry of C_{60} (I_h point group), however, there are only four characteristic modes possessing appreciable intensity. The mode with the highest intensity is assigned at the lowest wavenumber, 537 cm^{-1}. The CC stretching modes of C_{60} are assigned in the higher wavenumber region, 1460 and 1214 cm^{-1}. The calculated wavenumbers were scaled by a factor of 0.9613 as suggested by Merrick et al. [25]. The scale wavenumbers of C_{60} 516, 565, 1167 and 1404 cm^{-1} are in accordance with the FT-IR frequencies 526, 576, 1183 and 1429 cm^{-1}, respectively, as reported by Chase et al. [26]. The substitution of B_3N_3 into C_{60} leads to destruction of the sharpness of peaks in the IR spectrum due to C_3 point group. As seen in Fig. 2, a number of additional modes and mixing of various modes appear due to BN, BC and NC stretchings. For instance, the BN stretching modes appear at 1394 cm^{-1}. This mode possesses the strongest intensity due to charge transfer from B to N atoms. Furthermore, CC stretching modes of $B_3N_3C_{54}$ are shifted toward higher wavenumber region as compared to C_{60}. For example, the modes calculated at 1606 and 1586 cm^{-1} are assigned to CC stretchings with weak intensities. However, CC stretching and lower wavenumber mode of $B_3N_3C_{54}$ corresponding to C_{60} are obtained at 1468 cm^{-1} (medium) and 539 cm^{-1} (weak). On the contrary, Raman spectrum of $B_3N_3C_{54}$ closely resembles that of C_{60}. There are eight distinct modes of vibrations in the Raman spectra which are in accordance with the experimental reports of Bethune et al. [27, 28]. For instance, the most intense Raman peak calculated at 1465 cm^{-1} is observed at 1469 cm^{-1} in C_{60} solid film [27] and 1470 cm^{-1} in C_{60} thin film [28].

NMR spectra of $B_3N_3C_{54}$ and C_{60} are calculated by gauge independent atomic orbital (GIAO) approach at B3LYP/6-31G(d) level. The NMR relative chemical shifts of nucleus 'X' are calculated by $\delta = \delta_{ref} - \delta_{full}$, where δ_{full} are isotropic magnetic shieldings of nuclei of fullerene and δ_{ref} are those of reference systems which are $C_4H_{12}Si$ for C, B_2H_6 for B and NH_3 for N nucleus. The calculated chemical shift for C_{60} is 131.8 ppm whereas that of

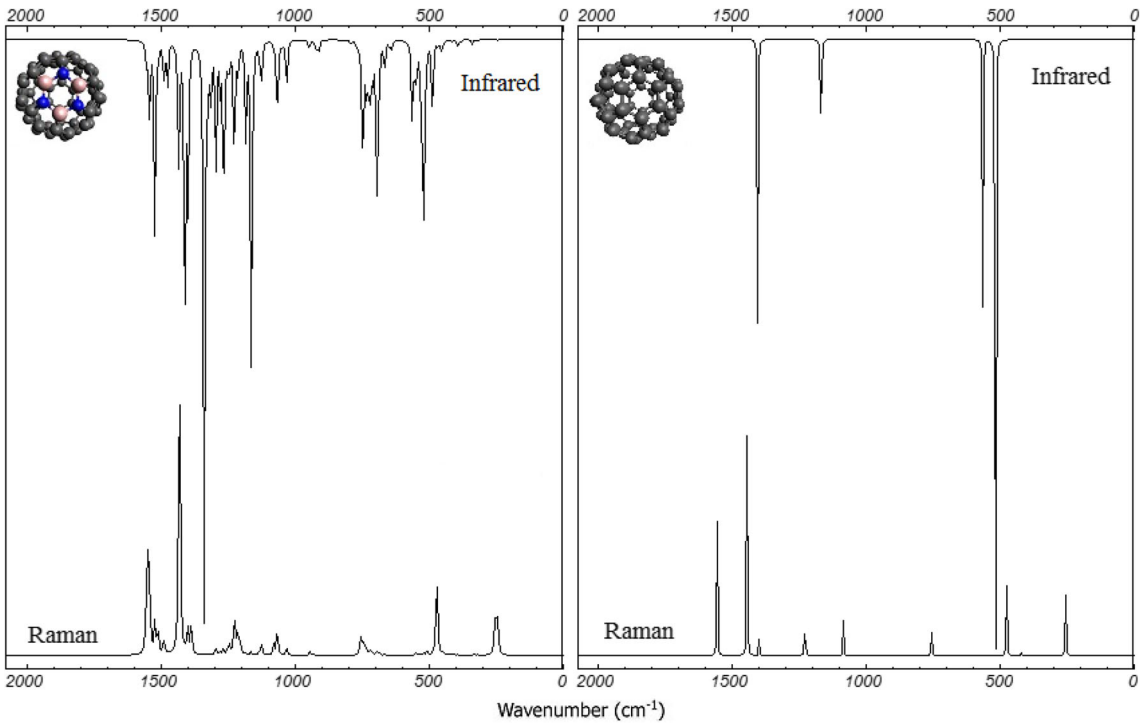

Fig. 2 Vibrational infrared and Raman spectra of $B_3N_3C_{54}$ and C_{60} calculated at B3LYP/6-31G(d) level

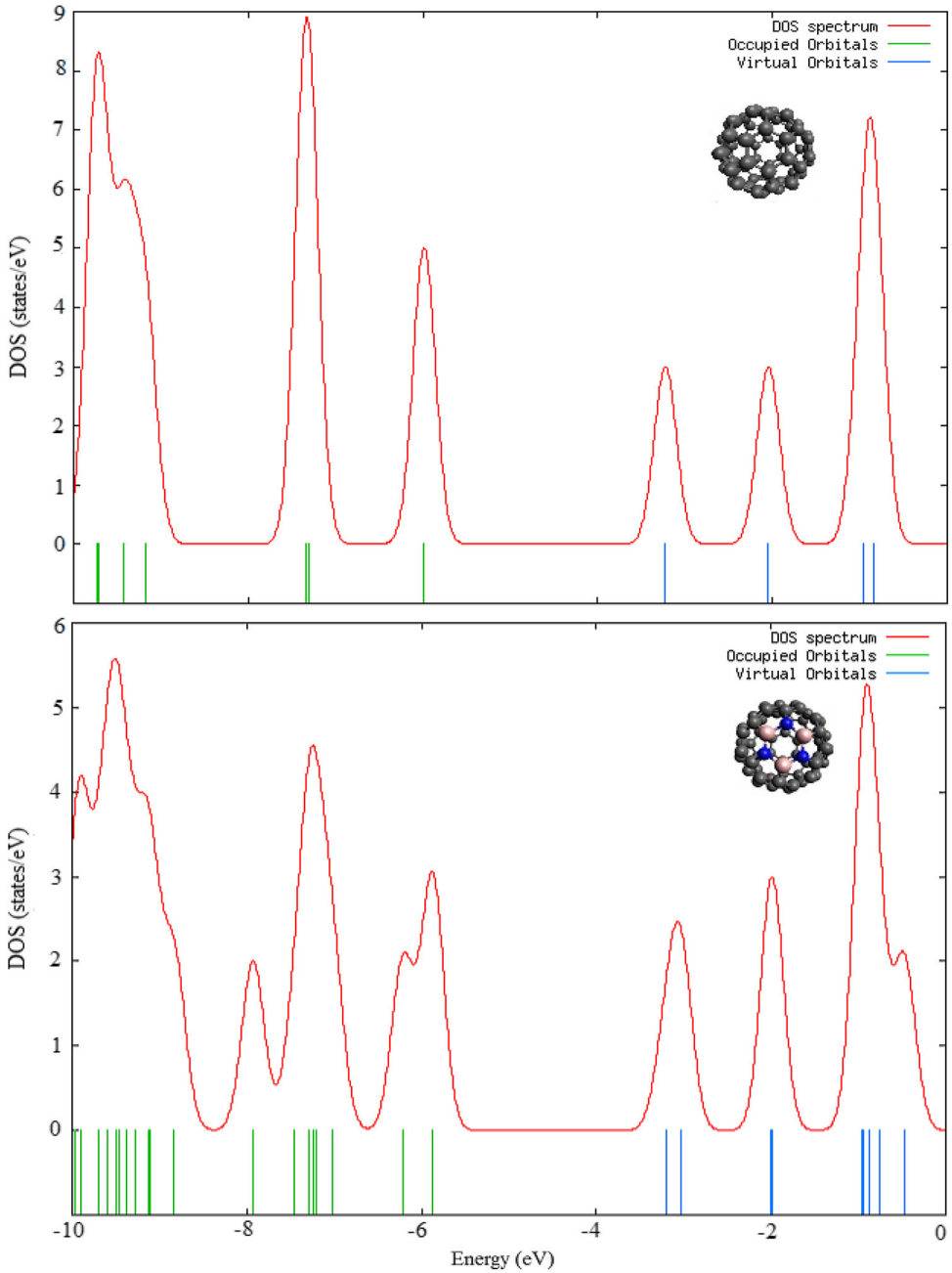

Fig. 3 Density of States (DOS) spectra of C_{60} and $B_3N_3C_{54}$ calculated at B3LYP level. Occupied (*green*) and unoccupied (*blue*) molecular orbital energy levels are also displayed

$B_3N_3C_{54}$ lies between 121.5 and 143.9 ppm. The minimal δ value corresponds to C attached to C–B bond whereas maximal value belongs to C bonded to C–N moiety, as expected due to lone pair of N atom. The triply degenerate NMR peaks of B and N nuclei in $B_3N_3C_{54}$ are found to be at 10.1 and 162.8 ppm, respectively.

Electronic properties

The density of states (DOS) spectra along with molecular orbital energy levels of $B_3N_3C_{54}$ and C_{60} are plotted in Fig. 3. One can note that the energy levels of the highest occupied molecular orbital (HOMO) and lowest unoccupied molecular orbital (LUMO) of $B_3N_3C_{54}$ are slightly shifted upwards relative to C_{60}. Furthermore, the substitution results in additional energy levels which are closely spaced and broaden the density of states spectrum. The DOS spectra also reveal that the HOMOs of C_{60} are five-fold degenerate and LUMOs are triply degenerate. This degeneracy of molecular orbitals is lowered for $B_3N_3C_{54}$ in which the HOMOs and LUMOs are triply and doubly degenerate, respectively. The degenerate HOMOs and

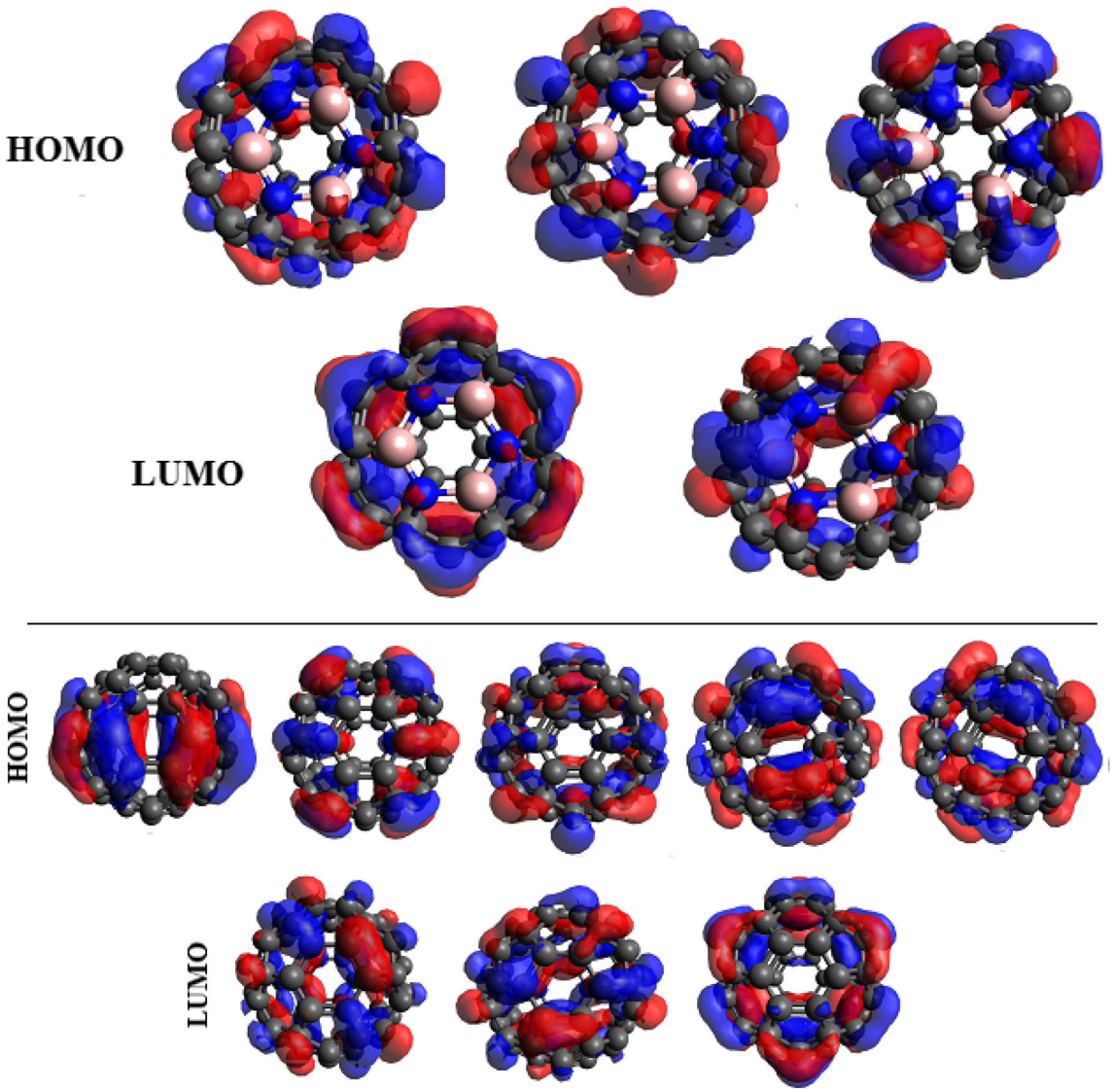

Fig. 4 Degenerate HOMOs and LUMOs of $B_3N_3C_{54}$ (*upper set*) and C_{60} (*lower set*)

Table 2 Electronic parameters of $B_3N_3C_{54}$ and C_{60} at B3LYP/6-31G(d) level

Parameter	$B_3N_3C_{54}$	C_{60}
$I = -E_{HOMO}$ (eV)	5.872	5.986
$A = -E_{LUMO}$ (eV)	3.205	3.228
$E_{gap} = E_{LUMO} - E_{HOMO} = I - A$ (eV)	2.667	2.758

LUMOs of $B_3N_3C_{54}$ and C_{60} are displayed in Fig. 4. Within the framework of Koopmans' theorem, the ionization potential (I) and electron affinity (A) are approximated by the negative energy eigenvalues of the HOMO and LUMO, respectively. From Table 2, one can note that the calculated I and A values of $B_3N_3C_{54}$ are lower than those of C_{60}. As known, it is energetically unfavorable to add electrons to a high-lying LUMO or to extract electrons from a low-lying HOMO and so to form the activated complexes of any potential reaction [29]. Therefore, $B_3N_3C_{54}$ is expected to be form cationic complexes due to smaller E_{HOMO} magnitude, i.e., I value than that of C_{60}.

The energy difference between HOMO and LUMO, HOMO–LUMO energy gap (E_{gap}) corresponds to the band gap in solids which is equal to the difference of I and A values. In molecular system, this energy gap is generally approximated to the chemical hardness [30]. This energy gap is equivalent to the energy required to free an outer shell electron which behaves as a mobile charge carrier that moves freely within the solid material. The E_{gap} is an important parameter that determines the electrical conductivity of a solid. Substances with larger energy gaps are

generally insulators, materials with smaller energy gaps are semiconductors, and conducting materials have very small or no energy gaps. In other words, the molecules with smaller energy gaps are less hard, and hence more reactive. Our calculated E_{gap} of C_{60} at B3LYP/6-31G(d) level (2.76 eV) is in agreement with the experimental band gap value of 2.3 ± 0.1 eV [31]. This energy gap being neither too large nor too small suggests the semiconducting behavior of C_{60}. In case of $B_3N_3C_{54}$, this energy gap is reduced to 2.67 eV. Therefore, the conductivity of $B_3N_3C_{54}$ should be slightly greater than that of C_{60}.

Conclusion

Using density functional theory-based calculations; we have studied the substitution of B_3N_3 hexagon into C_{60} fullerene. We noticed that the structure of $B_3N_3C_{54}$ closely resembles that of C_{60}. However, polar B–N bonds are weaker than that of covalent C–C bonds. The stabilization energy due to substitution of B_3N_3 into C_{60} is calculated to be 5.35 eV at B3LYP/6-31G(d) level. The vibrational infrared and Raman spectra of $B_3N_3C_{54}$ and C_{60} have been compared and it was noticed that the strongest peak in vibrational spectrum of $B_3N_3C_{54}$ is due to BN stretching and CC stretching modes are shifted to higher wavenumber region. The NMR chemical shifts of $B_3N_3C_{54}$ have also been computed. The density of states (DOS) spectrum of $B_3N_3C_{54}$ shows the reduction in the degeneracy of molecular orbitals, but enhancement in the peak width resulting in additional energy levels due to heteroatoms such that its HOMO–LUMO gap is reduced relative to C_{60}. This study should provide better insights into the surface modification of C_{60} by heteroatom.

Acknowledgments A. K. Srivastava, wishes to acknowledge Council of Scientific and Industrial Research (CSIR), India for financial help in the form of a senior research fellowship (SRF) [Grant No. 09/107(0359)/2012-EMR-I].

References

1. Langa, F., Nierengarten, J.-F. (eds.): Fullerenes Principles and Applications. RSC Publishing, Cambridge (2007)
2. Rao, C.N.R., Govindaraj, A.: Nanotubes and Nanowires. RSC Publishing, Cambridge (2005)
3. Misra, N., Dwivedi, A., Pandey, A.: Geometrical electronic, and vibrational properties of fullerene rings doped with transition metals. Chin. J. Phys. **50**, 64–72 (2012)
4. Dwivedi, A., Pandey, A.K.: Ab initio study of the endohedral fullerene $PbH_4@C_{60}$. Fuller. Nanotubes Carbon Nanostruct. **22**, 679–686 (2014)
5. Guo, T., Jin, C., Smalley, R.E.: Doping bucky: formation and properties of boron-doped buckminsterfullerene. J. Phys. Chem. **95**, 4948–4950 (1991)
6. Pradeep, T., Vijayakrishnan, V., Santra, A.K., Rao, C.N.R.: Interaction of nitrogen with fullerenes: nitrogen derivatives of C_{60} and C_{70}. J. Phys. Chem. **95**, 10564–10565 (1991)
7. Jensen, F., Toftlund, H.: Structure and stability of C_{24} and $B_{12}N_{12}$ isomers. Chem. Phys. Lett. **201**, 89–96 (1993)
8. Esfarjani, K., Ohno, K., Kawazoe, Y.: Band structure and chemical bonding in $C_{58}BN$ heterofullerenes. Phys. Rev. B **50**, 17830–17836 (1994)
9. Chen, Z., Ma, K., Chen, L., Zhao, H., Pan, Y., Zhao, X., Tang, A., Feng, J.: Theoretical studies on the substituted fullerenes $C_{60-x-y}B_xN_y$ ($x + y = 2$). J. Mol. Struct. Theochem. **452**, 219–225 (1998)
10. Krainara, N., Illas, F., Limtrakul, J.: Interaction of adenine Cu(II) complexes with BN-doped fullerene differentiates electronically equivalent tautomers. Chem. Phys. Lett. **537**, 88–93 (2012)
11. Siddiqui, S.A., Rasheed, T., Bouarissa, N., Al-hajry, A.: Possible use of BN-modified fullerene as a nano-biosensor to detect adenine–thymine Watson-Crick base pair in mutagenic tautomeric form: theoretical approach. J. Theor. Comput. Chem. **14**, 1550003 (2015)
12. Pattanayak, J., Kar, T., Scheiner, S.: Boron–Nitrogen (BN) substitution patterns in C/BN hybrid fullerenes: $C_{60-2x}(BN)_x$ ($x = 1-7$). J. Phys. Chem. A **105**, 8376–8384 (2001)
13. Pattanayak, J., Kar, T., Scheiner, S.: Boron–Nitrogen (BN) substitution of fullerenes: C_{60} to $C_{12}B_{24}N_{24}$ CBN ball. J. Phys. Chem. A **106**, 2970–2978 (2002)
14. Anafcheh, M., Hadipour, N.L.: A computational NICS and ^{13}C NMR characterization of BN-substituted ^{60}C fullerenes. Phys. E **44**, 400–404 (2011)
15. Liu, Z., Marder, T.B.: B–N versus C–C: How similar are they? Angew. Chem. Int. Ed. **47**, 242–244 (2008)
16. Srivastava, A.K., Misra, N.: The boron–carbon–nitrogen heterocyclic rings. Chem. Phys. Lett. **625**, 5–9 (2015)
17. Srivastava, A.K., Misra, N.: Introducing "carborazine" as a novel heterocyclic aromatic species. New J. Chem. **39**, 2483–2488 (2015)
18. Srivastava, A.K., Misra, N.: Heterocyclic $C_2B_2N_2H_6$ versus homocyclic C_6H_6. Main Group Chem. **14**, 369–375 (2015)
19. Frisch, M.J., et al.: Gaussian 09 Rev. B.01. Gaussian Inc., Wallingford, CT (2010)
20. Becke, A.D.: Density-functional exchange-energy approximation with correct asymptotic behavior. Phys. Rev. A **38**, 3098 (1988)
21. Lee, C., Yang, W., Parr, R.G.: Development of the Colle-Salvetti correlation-energy formula into a functional of the electron density. Phys. Rev. B **37**, 785 (1988)
22. Srivastava, A.K., Misra, N.: Novel planar chain like Li_7F_7 and Li_9F_9 nanostructures. Chem. Phys. Lett. **612**, 302–305 (2014)
23. Sikorska, C., Puzyn, T.: The performance of selected semi-empirical and DFT methods in studying C_{60} fullerene derivatives. Nanotechnology **26**, 455702 (2015)
24. Srivastava, A.K., Misra, N.: Structures, stabilities, electronic and magnetic properties of small Rh_xMn_y ($x + y = 2$–4) clusters. Comput. Theor. Chem. **1047**, 1–5 (2014)
25. Merrick, J.P., Moran, D., Radom, L.: An evaluation of harmonic vibrational frequency scale factors. J. Phys. Chem. A **111**, 11683–11700 (2007)

26. Chase, B., Herron, N., Holler, E.: Vibrational spectroscopy of C_{60} and C_{70} temperature-dependent studies. J. Phys. Chem. **96**, 4262–4266 (1992)
27. Bethune, D.S., Meijer, G., Tang, W.C., Rosen, H.J.: The vibrational Raman spectra of purified solid films of C_{60} and C_{70}. Chem. Phys. Lett. **174**, 219–222 (1990)
28. Bethune, D.S., Meijer, G., Tang, W.C., Rosen, H.J., Golden, W.G., Seki, H., Brown, C.A., de Vries, M.S.: Vibrational Raman and infrared spectra of chromatographically separated C_{60} and C_{70} fullerene clusters. Chem. Phys. Lett. **179**, 181–186 (1991)
29. Manolopoulos, D.E., May, J.C., Down, S.E.: Theoretical studies of the fullerenes: C_{34} to C_{70}. Chem. Phys. Lett. **181**, 105–111 (1991)
30. Pearson, R.G.: Chemical Hardness. Wiley-VCH, New York (1997)
31. Lof, R.W., van Veenendaal, M.A., Koopmans, B., Jonkman, H.T., Sawatzky, G.A.: Band gap, excitons, and Coulomb interaction in solid C_{60}. Phys. Rev. Lett. **68**, 3924 (1992)